

# Manganese Steel Castings: New Technology for Welding Frogs to Rail

M. BARTOLI and M. DIGIOIA

## ABSTRACT

Manganese steel frogs are normally connected to rails with the use of bolted fishplates because of the inability to weld the frog directly to the rail (as is normally done when connecting rails to each other). Described in this paper is a new process that makes the frog-to-rail connection possible by inserting an adapter casting that is flash-butt welded, first to the frog and then to the carbon-steel rail, thus eliminating the mechanical discontinuity between the parts to be connected. The chemical composition of the adapter casting is such that it can withstand, without embrittlement, the welding thermal cycle of the austenitic manganese steel of the frog and that of the carbon steel of the rail. In addition, it can undergo work hardening either before or after the installation, with a hardness between that of the frog and that of the rail. Unlike previously proposed techniques, this new process does away with the local deformation of the rail where the adapter is installed, which is a source of problems to the track and rolling equipment. Test sections of the proposed material have been flash-butt welded to both frog and rail ends with highly successful results.

Austenitic manganese steel has the well-known property of work hardening under repeated impact or other mechanical loading. Surface hardnesses of from 500 to 550 Brinell Hardness Number (BNH), depending on the carbon content, may be achieved while maintaining the typical toughness of the austenitic structure in areas away from the surface. For these reasons, austenitic manganese steel is widely employed as wear-resistant material under heavy-impact loading conditions.

Frogs for railway switches are often provided as austenitic manganese steel castings with a solution heat treatment. This heat treatment is necessary to eliminate embrittled precipitated carbides in the grain boundaries and the acicular carbides within the grains that developed during the slow cooling through the critical range of 800°C to 300°C following the pouring of the casting. A general relationship of the increase in brittleness of austenitic manganese steel versus the time-at-temperature is shown in Figure 1.

It is for this reason that manganese steel is not employed in services for which temperatures over 260°C are expected. Welding, therefore, is usually considered to be a hazardous operation with manganese steel and particularly so when extreme precautions are not taken to maintain a cold-welding procedure (1).

As a result, austenitic manganese steel frogs are normally connected to rails by the use of bolted fishplates for the preceding reasons. This causes a discontinuity at the frog-rail interface, which, in turn, results in increased wear of both the track and car wheels, especially on high speed railways.

The direct weld connection between manganese frogs and carbon steel rails cannot be carried out with the usual welding processes (e.g., thermit welding, shielded manual arc welding, etc.) nor with relatively modern processes such as flash-butt welding,

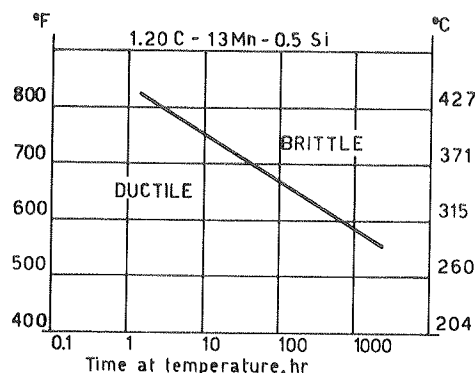


FIGURE 1 Time-temperature relationship for embrittlement of austenitic manganese steel.

which is widely employed in railway track applications.

This is due to the metallurgical incompatibility of the two steels. Rail carbon steel requires a slow cooling from the welding temperature to avoid brittle microstructures, while a slow cooling would produce serious amounts of carbide precipitation in austenitic manganese steel. Numerous unsuccessful methods, including other adapter designs, have been proposed to resolve the problem of joining the dissimilar steel components together. They all differ, however, as to the technique to be used to connect the adapter to the frog and rail, and as to the size and structure of the adapter itself. The following considerations should be taken into account in order to obtain the most reliable connection:

### 1. Material for the Adapter

The adapter must be of a quality that will enable it not to embrittle after welding, whether cooled rapidly or slowly.

• It must be able to work harden under repeated impact loading, so as to present a hardness intermediate between the materials it connects.

## 2. Dimensions and Shape of the Adapter

• Because the material components of the adapter are the most costly of all those under consideration, owing to their special properties, the adapter must be as short as possible. However, it must be long enough to ensure that neither of the two welds will have any thermal effect on the other.

• Because the frog/adapter/rail connection is essentially subjected to fatigue loading in service, the transverse cross section should have a profile similar to that of the rail to avoid stress concentrations resulting from sudden changes in shape.

## 3. Welding Characteristics

• Flash-butt welding is the most suitable procedure for this kind of application because of its rapidity, quality, reliability, and consistency, as well as the capability it offers to control the supply of heat and limit it to a restricted area.

• The utilization of this procedure permits butt welds without special and costly preparations on the end faces to be welded. For all the foregoing reasons, flash-butt welding is widely used in the railway industry to connect rails to each other.

## PROPOSED TECHNOLOGY

In accordance with the preceding considerations, the technology that the authors propose for connecting frogs to rails involves the following steps:

1. The redesign of the frog end to obtain a transverse section with a profile similar to that of the rail so that it can be flash-butt welded to the adapter. It should be noted in this regard that frogs designed by Breda Fucine Meridionali and used on the Italian railway network already have end sections with a profile that is similar to that of a rail, as shown in Figure 2. In order to be able to use the proposed technology for the "self-guarded" frogs designed in accordance with the American Railway Engineering Association (AREA) rules, it may be necessary to make some design changes, as schematically shown in Figures 3 and 4.

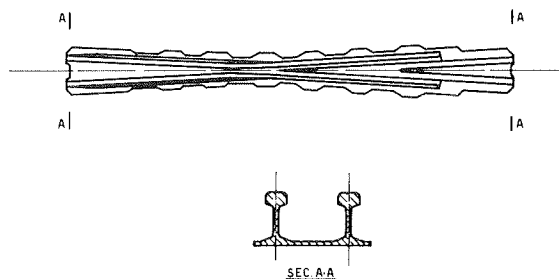


FIGURE 2 Italian railway frog.

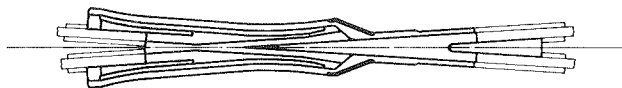


FIGURE 3 Self-guarded frog in accordance with AREA rules.

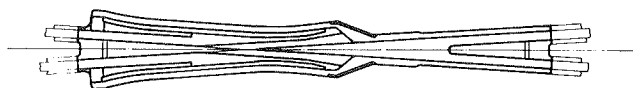


FIGURE 4 "Modified" self-guarded frog.

2. The production of an adapter, also with a profile similar to that of a rail, and with a length of between 100 and 200 mm. This length represents, in fact, a compromise between the two diverging requirements as to limiting the cost of the materials and allowing for sufficient distance between the two welds to avoid thermal effects of one weld on the other.

3. The use of the flash-butt welding technique for the joining of the adapters to the frog ends and rail ends. This will successively allow one to employ technology and equipment now used by the railroads.

4. The control of heat input, flash fumes, and quenching rate are important for successful frog-to-adapter welds as is the controlled cooling rate following the welding of the adapter-to-rail joint.

## EXPERIMENTAL RESULTS

To verify the validity of the proposed technology, a set of test samples and rail pieces, outlined in accordance with Union Internationale des Chemins de Fer 60 (UIC60), was prepared for the following materials:

1. Austenitic manganese cast steel, in the solution heat-treated condition, representative of the manganese frog;
2. Carbon steel for the rails, in an as-rolled condition;
3. High-alloy cast steel for the adapter, in a solution heat-treated condition.

All these samples have been flash-butt welded to each other under different conditions, with results that can be described as follows:

1. Base Material Properties. In Table 1, the main physical, chemical, metallurgical, and mechanical properties are summarized for the three types of materials. These properties have been obtained from samples A and C in a solution heat-treated condition with water cooling from 1100°C, and in an as-rolled condition for the rail, steel sample B.

2. Properties of the Weld Between A and C. For the purposes of determining the properties of this weld, samples were used that had square cross sections with 22 mm per side. These were flash-butt welded and cooled with water.

Bend tests, as identified by ASTM specification A 128, were made using a load perpendicular to the weld. In addition, impact tests on Masnager K-type specimens with a 2-mm U-notch on the fusion line as well as tensile tests of round specimens with welds at the center of the gage length were used for the evaluation. The results of the tests are given in Table 2 and are from specimens in an as-welded condition.

With respect to the base materials, the tensile test confirms that the weld does not diminish these mechanical properties. In fact, the tensile test fractures occurred in the C-type material at slightly higher ultimate values than were obtained from the unwelded C material without affecting the weld itself. The impact test values in the fusion zone were lower than those of the two base materials (A and C)

TABLE 1 Base Material Properties at Room Temperature

Material	Chemical Composition (%)		Mechanical Properties				
			Yield Strength [0.2% offset, in MPa (Ksi)]	Tensile Strength [MPa (Ksi)]	Elongation (%)	Impact K [J/cm <sup>2</sup> (ft lb)]	Hardness (BHN)
Type A (frog)	C	1.20					
	Mn	13.00	360	730	40	230	215
	Si	0.40	(52.2)	(105.8)		(136)	
Type B (rail)	C	0.45					
	Mn	1.00	540	780	18	35	220
	Si	0.20	(78.4)	(113.0)		(20.7)	
Type C (adapter)	C	0.15					
	Mn	6.00	295	575	50	150	190
	Si	1.80	(42.8)	(83.3)		(88.5)	
	Cr	23.00					
	Ni	13.00					

Note: C = carbon, Mn = manganese, Si = silicon, Cr = chromium, and Ni = nickel.

TABLE 2 Mechanical Properties at Room Temperature

Weld Type	Tensile Test		Elongation (%)	Failure Location	Impact K [J/cm <sup>2</sup> (ft lb)]	Bend ( $\alpha^\circ$ )
	Yield Strength [0.2% offset, in MPa (Ksi)]	Tensile Strength [MPa (Ksi)]				
A-C	310 (44.9)	580 (84.0)	42	Failed in C material	80 (47.2)	80
B-C	290 (42.1)	580 (84.0)	38	Failed in C material	30 (17.7)	80

connected together; however, the results were still significantly higher than those of the base rail material. The bend test, however, during which the first cracks appeared at approximately 80 degrees, showed that the fracture presented totally ductile features.

Rotating fatigue tests were also carried out in accordance with (DIN) Specification 50113. The results indicated a fatigue limit exceeding 220 N/mm<sup>2</sup>. All specimens had the weld at the center of their gage length and broke in the C-type material at distances greater than 10 mm from the fusion line, thus indicating that the weld performed well when subjected to fatigue.

The research was completed with a microscopic examination that showed a negligible amount of carbide precipitation at the grain boundaries and within the grains of the austenitic manganese steel. An increase in carbide precipitation occurred on the C material side of the weld between the A and the C materials (Figure 5). This latter precipitation is the result of the significant difference between the carbon contents of the two materials, and, as the results of the tests clearly demonstrate, does not cause a reduction in the property values of the weld. On the contrary, a series of tests performed on specimens that were solution heat-treated after welding showed a drop in the impact properties, with average values of only 4 J/cm<sup>2</sup>, notwithstanding the microscopic study, which showed an absence of the carbide precipitation line.

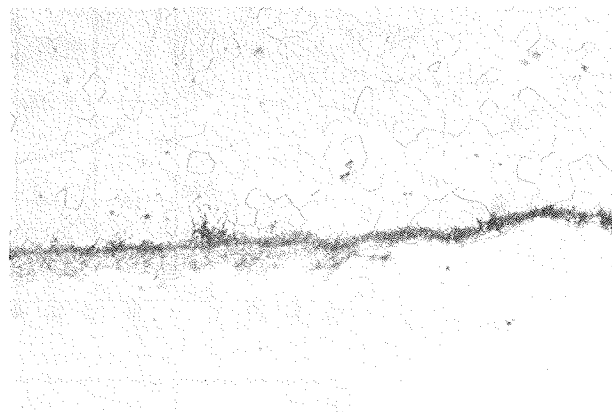
3. Properties of the Weld Between B and C. Similar to the tests performed on the weld joining materials A and C, a second series of tests was carried out on specimens obtained by flash-butt welding material B with material C and controlling the post-weld cooling by sending current impulses through the joint. The results of these tests are summarized in Table 2.

This weld also shows mechanical properties comparable to those of the materials welded: the bend and impact test values are influenced by the carbon steel properties of the rail. During the course of the bend test, the fracture of the B-C joint started after approximately 80 degrees and involved only material B, without affecting the fusion area.

The rotating bend fatigue tests confirmed the results obtained on the weld linking materials A and C. The microscopic study revealed an absence of brittle structures on the carbon steel rail side of the weld.

4. Weld between Rail Specimens with an Outline in Accordance with UIC60 and Materials A, B, and C.

"A" Steel



"C" Steel

FIGURE 5 Micrography of A-C welding (75x).

For the purposes of verifying the effectiveness of the technology proposed in the present paper, studies on the small samples were followed with tests on welds connecting specimens of rail having an outline conforming with UIC60.

#### Bend Tests

These bend tests were performed in accordance with the provisions of the Italian Railway Rules to verify the quality of the flash-butt weld between the rails. The values of the resulting deflection, measured over a length of 1 m and obtained before cracks began to appear on the flange, were (a) weld between A and C materials:  $\geq 60$  mm; and (b) weld between B and C materials:  $\geq 40$  mm. (It must be noted, however, that the minimum deflection value required for the acceptance of flash-butt welds between rails is 25 mm.)

#### Plain Pulsating Bending Fatigue Tests

Two plain pulsating bending fatigue tests were performed in accordance with the loading configuration reproduced in Figure 6, using a load varying from 30 to 300 kN to verify the manner in which the proposed procedure reacted to fatigue.

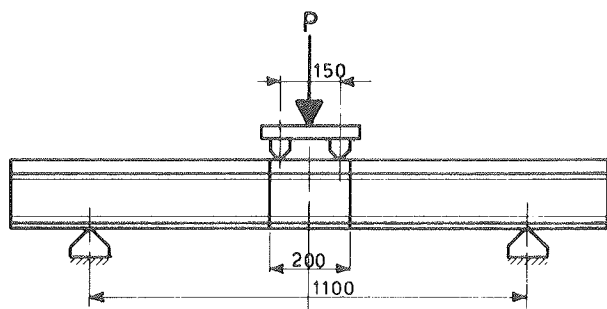


FIGURE 6 Fatigue test configuration.

The two joints presented a fracture initiation after  $1.5 \times 10^6$  and  $2.5 \times 10^6$  cycles, respectively; in both cases, the fracture occurred at approximately 10 mm from the fusion line of the A-type material, which simulated the frog cast in manganese steel.

This result, considering also the rotating bending fatigue tests carried out on specimens and previously described, leads the authors to attribute the cause of the fracture to defects already existing in the manganese steel, and not to weakness factors induced by the weld itself. This was also confirmed by the results of a fractometric and microscopic study done on the fracture face. The propagation of the fracture occurred slowly, an indication of the toughness of the joint structure.

#### Verification of the Size Effect

Samples were taken from the weld zone of actual rail specimens for tensile, impact, bending, and rotating bending tests. The results of these tests confirmed the data obtained from the tests described previously.

#### Verification of the Work Hardening of Material C

As stated earlier, a primary goal of the proposed technology lies in the ability of the adapter to harden on impact loading, or to undergo prework hardening before installation when subjected to one of the techniques usually adopted for austenitic manganese steel. Also, it is necessary for the adapter to have a hardness intermediate between that of the cross-frog and that of the rail.

TABLE 3 Surface Hardness After Explosion

Material	No Shot (BHN)	One Shot (BHN)	Two Shots (BHN)	Three Shots (BHN)
Type A	215	315	352	388
Type C	190	225	245	265

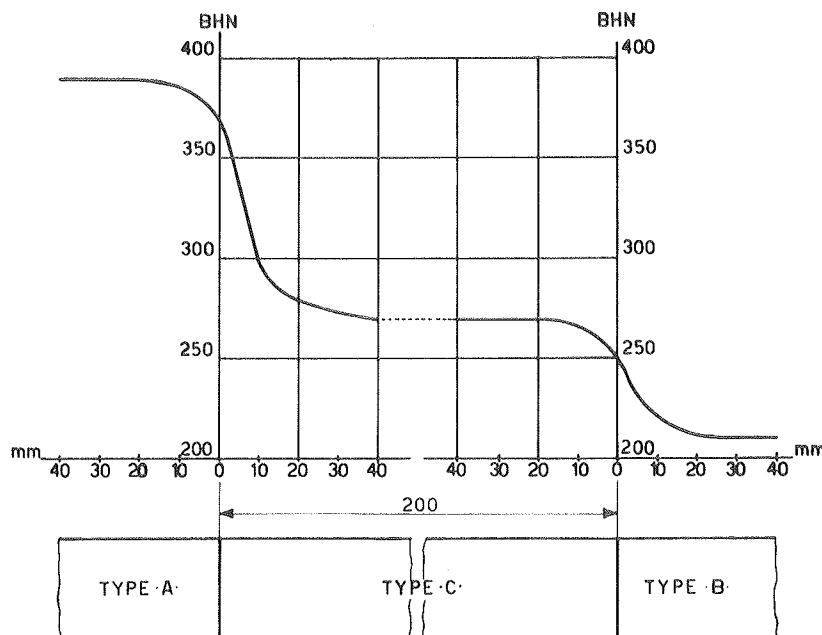


FIGURE 7 Hardness trend after explosion hardening.

Because data relative to parts already in service were not available, explosion hardening tests were performed to verify the soundness of the preceding affirmations. The results obtained on the A- and C-type steels are summarized in Table 3.

The extent to which the C material of the adapter will harden varies from 190 BHN for the solution heat-treated material to 265 BHN after three explosions. As expected, it thus presents a hardness that is intermediate between the hardened cross-frog and that of the rail.

Figure 7 schematically shows the hardness trend close to the two welds and along the adapter.

It must be noted that a special microscopic study showed that the hardening of the adapter must be traced back not so much to sliding planes, as occurs in austenitic manganese steel, but to the fragmentation of large austenite grains into smaller and more numerous ones.

## CONCLUSIONS

A new technology has been presented in this paper that permits the connection of the manganese frog to

the rail without mechanical discontinuities, and that overcomes limitations arising from other similar proposals. In addition, a series of successful results has been presented from tests performed at Breda Fucine Meridionali on flash-butt welds between experimental samples and between specimens of actual track materials.

The results obtained allow the authors to affirm that the proposed process is extremely reliable and has met all of the initial objectives. Other materials, also patented in Italy, are presently being tested at the authors' plant in Bari.

## REFERENCE

1. M. Bartoli. Welding Filler Metal (Materiale d'apporto nella saldatura). Il Gionale dell'Officina, No. 3, Milan, Italy, March 1985.

Publication of this paper sponsored by Committee on Railroad Track Structure System Design.

# Evolution of the Rail-Bound Manganese Frog

E. E. FRANK

## ABSTRACT

During the 19th century, the railroad frog was fabricated from standard carbon steel rail. During this period, there were many designs for the rigid frog from riveted plate frogs to the current AREA standard rigid frog. In the late 1800s, however, R.A. Hadfield of England developed "Hadfield Manganese Steel." The unusual properties of this manganese steel, as well as its toughness and ability to withstand severe impacts, made it most suitable for railroad service. The first manganese steel castings were made for street railway frogs. The success of manganese steel in the street railway castings led to its use in steam railway special work frogs, crossings, and switches. By the first decade of the 20th century, the rail-bound frog was introduced to the American railroads. Since then, the rail-bound manganese frog has progressed through many design improvements. Currently, there are new designs being developed to meet the needs of the heavy-haul railroad.

The rail-bound manganese frog evolved from the need to greatly improve the life of the rail-built frog, which was the standard frog used during the 19th century. During this period, the rail-built frog was manufactured from Bessemer steel in a variety of designs (i.e., riveted plate rigid frogs, clamp-type rigid frogs, bolted rigid frogs with cast iron

fillers, and, in later years, with rolled steel fillers).

## MANGANESE STEEL IN SPECIAL TRACKWORK

During this era, Bessemer rail-built frogs installed in severe locations would last on the average of 3 months. The industry recognized that the Bessemer rail-built frog was a high-maintenance, high-cost track component, and that a product having both